Pressure and density dependence of the boson peak in polymers

L. Hong,[1] B. Begen,[1] A. Kisliuk,[1] C. Alba-Simionesco,[2] V. N. Novikov,[3] and A. P. Sokolov[1,*]
[1]*Department of Polymer Science, The University of Akron, Akron, Ohio 44325-3909, USA*
[2]*Laboratoire de Chimie Physique, UMR 8000, CNRS, Universite' Paris Sud, 91405 Orsay, France*
[3]*Institute of Automation and Electrometry, Russian Academy of Sciences, Novosibirsk, 630090, Russia*
(Received 10 July 2008; revised manuscript received 15 September 2008; published 8 October 2008)

The nature of the low-frequency vibrations, the so-called boson peak, in spectra of glass-forming systems remains a subject of active discussions. It appears that densification of glasses leads to significant change of the boson peak vibrations and opens additional possibility to verify different model predictions. We present light (Raman and Brillouin) scattering studies of the influence of pressure (up to 1.5 GPa) on the boson peak vibrations and elastic properties of five different polymers. We demonstrate that the pressure-induced shift of the boson peak frequency in all cases is significantly stronger than change of sound velocities. This result clearly shows the failure of the homogeneous elastic continuum approximation. The boson peak amplitude decreases strongly with pressure. However, the major part of these variations (but not all) can be related to the change of the Debye level. We emphasize a correlation between pressure-induced variations of the boson peak frequency and intensity. Surprisingly, the spectral shape of the boson peak remains the same at all pressures indicating that the frequency distribution of the vibrational modes remains essentially unaltered even when the boson peak frequency doubles. The results are compared to predictions of different models and results of recent computer simulations.

DOI: 10.1103/PhysRevB.78.134201 PACS number(s): 61.43.Fs, 63.50.−x, 64.70.P−

I. INTRODUCTION

Understanding the microscopic nature of the fast dynamics, i.e., molecular dynamics in the GHz–THz frequency range in disordered materials remains a challenge. Spectra of fast dynamics in amorphous materials deviate strongly from the expectations of the Debye model.[1] The latter assumes homogeneous elastic continuum and usually describes well the density of vibrational states $g(\nu)$ in crystalline materials in the GHz–THz frequency range. However, all disordered systems, including glasses and polymers, have two extra contributions in comparison to the Debye density of vibrational states $g_{\mathrm{Deb}}(\nu)$: (i) an anharmonic relaxation-like contribution that appears as a broad quasielastic scattering (QES) in light and neutron scattering spectra[2–4] and (ii) a harmonic vibration contribution which appears as a broad peak, the so-called boson peak, in light and neutron scattering spectra.[2–4] Although the boson peak is observed in spectra of almost all disordered systems, the microscopic nature of these excess vibrations remains a subject of active discussions.[5–18] There are essentially three main approaches to description of the boson peak vibrations: (i) particular vibrations localized (or quasilocalized) in specific (defect-like) places of the disordered structure, e.g., soft potentials and interstitials;[5–8] (ii) strong scattering of acoustic-like modes on elastic constants fluctuations in disordered structure,[9–11,13] and (iii) modes localized on some nanoscale blobs that are assumed to exist in disordered structures.[12] There are many experimental arguments in favor and against of all these approaches that help theoreticians to modify and develop deeper understanding of the microscopic nature of the boson peak.

It is known that the strength of the boson peak in glasses measured relative to the expected Debye level, $A_{\mathrm{BP}}=g(\nu_{\max})/g_{\mathrm{Deb}}(\nu_{\max})$, depends significantly on chemical structure of the system: it is high in network glasses and it is relatively weak in many van der Waals and ionic systems.[13,19,20] The boson peak appears to be also sensitive to the molecular weight in polymers[21–23] and quenching and densification of glass-forming systems.[14,24–32] All these dependences help to unravel the microscopic parameters of disordered structure that affect the boson peak vibrations. In particular, application of external pressure (densification) modifies the spectra of the boson peak significantly:[14,27–32] its frequency ν_{BP} increases and the measured amplitude I_{BP} decreases with increase in pressure. The reverse has been observed for quenched samples.[24–26] These kinds of studies provide advantages in analyzing the boson peak variations without chemical modification of the samples and in this way open a possibility for thorough tests of various models.[14,27–32]

One of the main problems in these studies is that the pressure and quenching affect many other properties of the material, including elastic constants (sound velocity) and density. As a result, direct comparison of the experimental data on the boson peak variations to model predictions should include changes in these parameters into account. So, the measurements of the boson peak should be accompanied by the parallel measurements of other important parameters. Recent analysis of nuclear inelastic scattering suggests[14,26] that the main variations of the boson peak after compression and pressure release and also upon quenching follow the expected variations of the elastic continuum, i.e., the boson peak frequency follows the variations of the sound velocity and the amplitude of the boson peak decreases proportional to the variations of the Debye level, i.e., the A_{BP} remains constant. However, detailed analysis of the fast dynamics in poly(isobutylene) (PIB) clearly demonstrates that the elastic continuum fails in this case.[31] Also, earlier data on some oxide glasses show clear difference in changes of the boson peak frequency and sound velocity,[28] and analysis of the bo-

son peak amplitude in chalcogenide glasses also reveals that its amplitude relative to the expected Debye level increases under pressure.[27] Thus some contradictions are reported in literature.

The current paper presents studies of the variations of the fast dynamics under pressure in five different polymers using light scattering (Raman and Brillouin) techniques. In all cases the boson peak frequency increases with pressure much stronger than sound velocity, consistent with earlier observations reported in Refs. 28 and 31. The boson peak amplitude decreases strongly with pressure. However, the major part of these variations (but not all) can be related to the change of the Debye level. We emphasize a correlation between pressure-induced variations of the boson peak frequency and intensity. Surprisingly, the spectral shape of the boson peak remains the same indicating that the frequency distribution of the vibrational modes remains essentially unaltered. Both observations are consistent with the earlier data for PIB presented in Ref. 31.

II. EXPERIMENT

All five polymers used in our studies were purchased from commercial sources: 1,2-polybutadiene (PBD), >85% of 1,2 content, with M_w=112,500 g/mol and M_n=104,000 g/mol, Tg=269 K (Polymer Source); poly(methylphenyl siloxane) (PMPS) with M_w =25,600 g/mol, M_n=15,800 g/mol, Tg=247 K (Polymer Source); oligomer of polystyrene (PS) with M_w =580 g/mol, M_n=540 g/mol, Tg=253 K (Scientific Polymer); polyisoprene (PIP) with M_w=2,450 g/mol, M_n =2,410 g/mol, Tg=201 K (Scientific Polymer), and polyisobutylene (PIB) with M_w=3,580 g/mol, M_n =3,290 g/mol, Tg=195 K (Polymer Standard Service). The samples were placed in a commercial anvil pressure cell (from D'Anvils), which can achieve pressure higher than 2 GPa. Both diamond and moissanite were used as anvil materials. The pressure in the anvil cell has been changed at room temperature. Thus all the samples compressed in these conditions are crossing their glass transition lines at a particular pressure above atmospheric P, and for all the samples studied here the highest compression was applied to solid polymers. The anvil cell was placed in an optical cryostat (Janis ST-100 model) for temperature variations. The measurements were performed at 140 K (i.e., far below Tg for all the samples).

The shift of the photoluminescence peak of ruby at wavelength around 690 nm was used to estimate the pressure inside the cell. We used two pieces of ruby: one was placed inside the sample, and the other one was attached to the outside surface of the cell. This design compensates the effect of temperature on the photoluminescence peak shift and allows very accurate measurements of pressure inside the sample cell at any T. Additionally, we used mercury lamp for precise measurements of the wavelength, and the final accuracy of the pressure estimates was better than 0.05 GPa.

Single-mode Ar+ ion laser (Lexel 3500) with wavelength 514.5 nm and ~20–40 mW power on a sample was employed for the light scattering measurements. The angle between the incoming laser light and the scattered light was 90 degrees and the sample plane was crossing this angle in the middle, i.e., was at 45 degrees relative to both incoming and scattering light directions. This is the so-called symmetrical scattering geometry that has the advantage to compensate the refractive index and to exclude the influence of its pressure variations on the final results.[33] Brillouin scattering spectra were measured using a tandem Fabry-Pérot interferometer (Sandercock model) with two different free spectral ranges, 50 and 375 GHz. Longitudinal Brillouin modes were measured in polarized spectra. Depolarized scattering spectra were used to measure transverse acoustic modes and the quasielastic spectra. The Raman spectra were measured using a Jobin Yvon T64000 triple monochromator in a subtractive mode. The polarized Raman spectra were used to estimate the sample temperature from the ratio of the Stokes and anti-Stokes intensities. Depolarized Raman spectra down to frequency $\nu \sim 100-200$ GHz (good overlap with the tandem data) were used to analyze the boson peak and microscopic peak spectra. The intensity of the combined (Raman plus tandem) depolarized scattering spectra were normalized at high-frequency optical modes in the range $\nu \sim 4-11$ THz. This normalization provides intensity per mole of the sample.

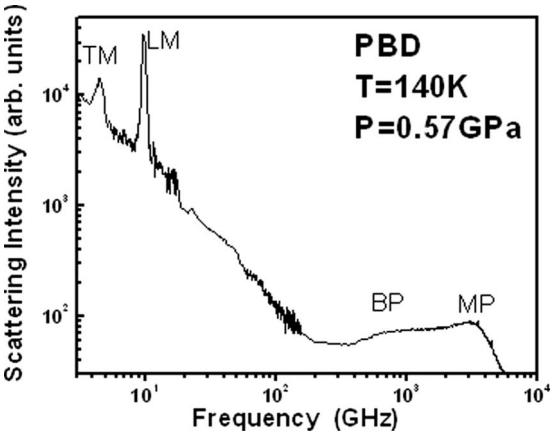

FIG. 1. Depolarized light scattering intensity measured on PBD at T=140 K and P=0.57 GPa. The spectrum shows transverse Brillouin mode (TM), longitudinal Brillouin mode (LM, leak of intensity due to nonperfect polarization scheme), the boson peak (BP), and the microscopic peak (MP).

III. RESULTS AND THEIR ANALYSIS

The measured light scattering spectra (Fig. 1) show three types of vibrational modes: (i) Brillouin peaks at $\nu \sim 5-15$ GHz that corresponds to transverse (TM) and longitudinal (LM) acoustic modes, (ii) the boson peak (BP) at $\nu \sim 700-900$ GHz, and (iii) microscopic peak (MP) between about 2 and 3 THz that presents an end of the acoustic-like band. All three modes change significantly their frequency and intensity under pressure.

The Brillouin peaks at different pressures were fitted by a simple Lorentzian function (Fig. 2) to estimate the frequency of the longitudinal ν_{LA} and transverse ν_{TA} Brillouin modes.

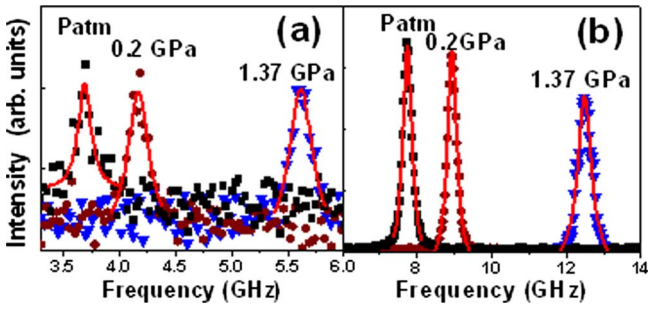

FIG. 2. (Color online) Brillouin scattering spectra of PIP at 140 K at different pressures: (a) Transverse modes; (b) Longitudinal modes. Symbols—experimental data and lines are the fits by a Lorentzian function.

These frequencies were used to estimate the corresponding sound velocity, V_{LA} and V_{TA}, using expression for the symmetric scattering measured at $\theta=90°$:

$$V_x = \frac{\lambda \nu_x}{2\ \mathrm{Sin}\dfrac{\theta}{2}}; x = \mathrm{TA,LA}. \tag{1}$$

Here $\lambda=514.5$ nm is the wavelength of light. To analyze the frequency and intensity of the boson peak, we present the data as a spectral density that takes into account thermal population of vibrational modes:

$$I_n(v) = \frac{I(v)}{v[n(v)+1]}. \tag{2}$$

Here $n(\nu)=[\exp(h\nu/kT)-1]^{-1}$ is the Bose temperature factor and $I(\nu)$ is the measured intensity. Figure 3 shows the boson peak spectra of PIP at various pressures. An increase in pressure leads to a shift of the boson peak maximum ν_{BP} toward higher frequency and a decrease in its amplitude. For the quantitative analysis, the spectra were fitted by a previously proposed expression,[34]

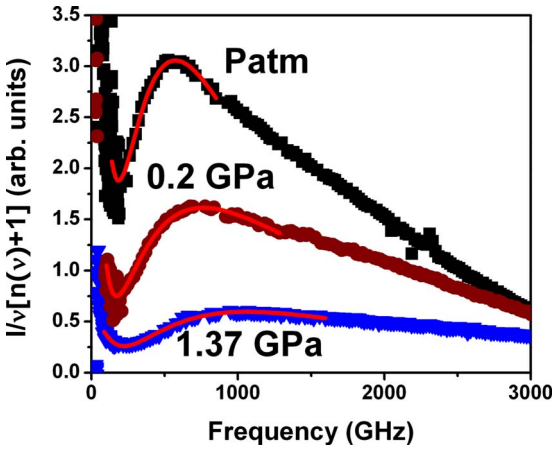

FIG. 3. (Color online) Depolarized light scattering spectra of PIP presented as a spectral density at $T=140$ K and three different pressures indicated in the plot: Symbols are experimental data and lines are fits with Eq. (3).

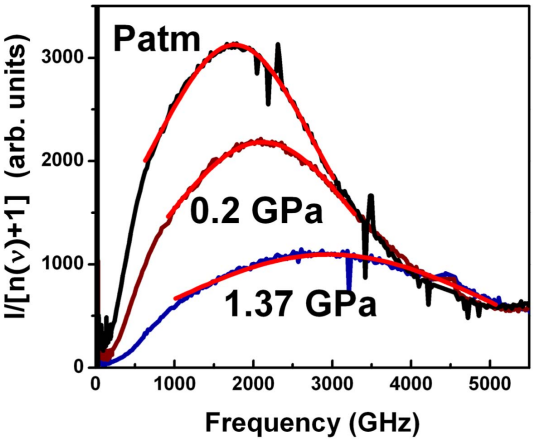

FIG. 4. (Color online) Microscopic peak in PIP (spectra presented as the susceptibility for more clear observation of the peak): Symbols are experimental data and lines are the fits by a Lorentzian function.

$$I_n(v) = \frac{Av_0}{v_0^2+v^2} + B\ \exp\left\{-\frac{[\ln(v/v_{\mathrm{BP}})]^2}{2W^2}\right\}, \tag{3}$$

where the first term describes the quasielastic contribution presented by a Lorentzian function with width ν_0 and amplitude A, and the second term describes the boson peak approximated by a log-normal function with a width W, an amplitude B, and a peak frequency ν_{BP}, both terms are assumed to be statistically independent. The frequency of the microscopic peak was analyzed in susceptibility presentation, $\chi''(\nu)\propto I_n(\nu)^*\nu=I(\nu)/[n(\nu)+1]$, where it is better visible (Fig. 4). This peak also shifts to higher frequency and decreases in amplitude with increasing pressure. To estimate the frequency of the microscopic peak ν_{MP}, we fit the susceptibility spectra around the maximum by a simple Lorentzian (Fig. 4). The data obtained from the fit for all five polymers are presented in the Table I. We emphasize that due to very strong quasielastic scattering, spectra of PBD and PMPS at ambient pressure do not exhibit a clear boson peak even at $T=140$ K. The boson peak is covered by the high-frequency tail of the quasielastic scattering. So we were not able to estimate ν_{BP} at ambient pressure with a reasonable accuracy in these polymers.

IV. DISCUSSION

A. Estimates of the density variations

The calculated sound velocity (Table I) can be used for direct estimates of the density variations in the samples under pressure.[35] The density variations can be expressed as

$$\left(\frac{\partial\rho}{\partial P}\right)_T = \left(\frac{\partial\rho}{\partial P}\right)_S + \alpha\rho\left(\frac{\partial T}{\partial P}\right)_S. \tag{4}$$

Here α is the thermal expansion coefficient, ρ is the density, and S is the entropy. This equation can be expressed in terms of the measured sound velocities:

TABLE I. Frequency of various modes as a function of pressure at $T=140$ K for the five studied polymers. (ν_{BP}, ν_{MP}, ν_{LA}, and ν_{TA} are the frequency of the boson peak, microscopic peak, longitudinal, and transverse Brillouin modes, respectively.) Also, longitudinal (V_{LA}) and transverse (V_{TA}) sound velocities and density values calculated from the Brillouin spectra are presented. Accuracy of the density data is $\pm 2\%$.

Sample	Pressure (GPa)	ν_{BP} (GHz)	ν_{MP} (GHz)	ν_{LA} (GHz)	ν_{TA} (GHz)	V_{LA} (km/s)	V_{TA} (km/s)	Density (g/cm^3)
	0.0001	725	2635	9.27	4.82	3.37	1.75	0.964
	0.08	803	2675	9.39	4.87	3.42	1.77	0.976
	0.3	992	2914	11.08	5.62	4.03	2.04	1.002
PIB	0.55	1091	3013	12.02	6.07	4.37	2.21	1.026
	0.74	1176	3198	12.79	6.41	4.65	2.33	1.041
	1	1262	3380	13.47	6.75	4.90	2.46	1.059
	1.37	1271	3374	14.09	6.98	5.13	2.54	1.083
	0.0001	605	1791	7.78	3.70	2.83	1.35	1.011
	0.10	675	1888	8.15	3.99	2.97	1.45	1.030
	0.20	779	2112	8.98	4.23	3.27	1.54	1.046
PIP	0.60	919	2382	10.41	4.92	3.79	1.79	1.095
	0.90	1008	2580	11.32	5.17	4.12	1.88	1.124
	1.10	1064	2702	11.81	5.38	4.30	1.96	1.141
	1.37	1131	2855	12.51	5.67	4.55	2.06	1.162
	0.0001	518	2411	7.61	3.66	2.77	1.33	1.066
	0.14	581	2626	8.32	3.89	3.03	1.42	1.091
PS	0.55	677	2926	9.43	4.28	3.43	1.56	1.150
	0.88	748	3115	10.34	4.60	3.76	1.67	1.188
	1.2	862	3467	11.31	4.96	4.12	1.80	1.218
	1.54	890	3674	11.81	5.15	4.30	1.87	1.246
	0.0001							1.240
	0.047	310	2431	7.04	3.53	2.56	1.28	1.252
PMPS	0.4	416	3034	8.73	4.05	3.18	1.47	1.320
	0.95	525	3472	10.03	4.57	3.65	1.66	1.388
	1.32	643	4058	11.18	5.08	4.07	1.85	1.427
	0.0001		2754	6.78		2.47		0.960
	0.07	658	2942	8.25	4.00	3.00	1.46	0.974
	0.32	792	3078	8.98	4.17	3.27	1.52	1.012
PBD	0.57	906	3271	9.97	4.63	3.63	1.68	1.045
	0.8	1015	3472	10.87	5.04	3.96	1.83	1.069
	1.12	1197	3974	12.42	5.75	4.52	2.09	1.096
	1.37	1323	4135	12.99	6.16	4.73	2.24	1.113

$$\left(\frac{\partial \rho}{\partial P}\right)_T = \frac{1}{V_{LA}^2 - \frac{4}{3}V_{TA}^2} + \frac{\alpha^2 T}{C_P}. \quad (5)$$

Here C_P is the specific heat. Thus, the pressure-induced change in density, $\Delta\rho(P)$, can be estimated by integrating Eq. (5) and using the measured sound velocities.[35] The second term in Eq. (5), $\alpha^2 T/C_p$, is much smaller than the first term. For example, the second term is about 8% of the first one for PS at 140 K and ambient pressure,[36,37] and this ratio does not change much with pressure.[35] So we assume that the second term provides additional 8% of the first term for all the samples independent of pressure. This assumption will add an extra error ~1% to the final estimated density.

Using Eq. (5) we can only estimate the variation of density $\Delta\rho(P)$. In order to get absolute values of density, we need to know the density of the material at ambient pressure, ρ_0. We were not able to find in the literature ρ_0 at $T=140$ K for all the polymers studied here. Thus, in order to estimate the initial density ρ_0, we (i) extrapolated the known density at ambient pressure from room temperature to Tg using known thermal expansion coefficient in the liquid state, and then (ii) extrapolated the density from Tg to T

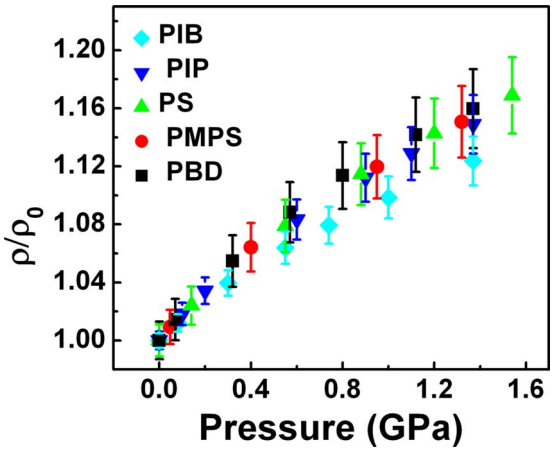

FIG. 5. (Color online) Pressure variations of relative density at 140 K calculated for all the studied polymers using Brillouin scattering data; ρ_0 is the density at ambient pressure.

=140 K using thermal expansion coefficient in the solid state.[38] This procedure provides additional uncertainty for the calculation of the absolute density. However, the resulting calculation of the relative variations of density, $\Delta\rho(P)/\rho_0$, will keep reasonable error bars, comparable to error bars coming from other sources (accuracy of the measurements and of the approximation used). We estimate the final accuracy for the relative density to be better than 2%.

The calculated relative density in all polymers shows slightly sublinear variations with pressure, reaching $\Delta\rho(P)/\rho_0 \sim 12-17\%$ at $P \approx 1.5$ GPa (Fig. 5). It is interesting to note that PIB has the smallest density changes, while PBD has the largest variations. We emphasize that compression of PIB up to $P \sim 0.8$ GPa occurs in a liquid state, while PBD is compressed mostly in the glassy state (due to its higher Tg). So if compression of both polymers would be in a liquid phase, the difference in change of density will be even higher. This difference in variation of $\Delta\rho(P)/\rho_0$ agrees with the recent theoretical works[39] connecting fragility to frustration in packing of polymer chains. According to Dudowicz *et al.*,[39] strong (in terms of fragility) polymers are well packed, while fragile systems have strong frustration in packing. Following this idea one would expect higher compressibility (larger variations in density under pressure) for more fragile polymers. Indeed, PBD is one of the most fragile among the polymers studied here,[40] while PIB is the least fragile one.[41,42]

Equation (5) can also be written as

$$\frac{d \ln \rho}{dP} = 1/K(P), \tag{6}$$

where $K(P)$ is the isothermal bulk modulus. In a good approximation, $K(P)$ varies linearly with pressure, $K(P)=K_0+K_1P$, and thus

$$\rho = \rho_0\left(1 + \frac{K_1}{K_0}P\right)^{1/K_1}. \tag{7}$$

We note that our Brillouin scattering data provide adiabatic moduli. The difference between the adiabatic and isothermal modulus deep in the glassy state is small and can be related to the same term $\alpha^2 T/C_p$ [Eq. (5)]. As we discussed above, this term is much smaller than $1/V_{\mathrm{LA}}^2 - \frac{4}{3}V_{\mathrm{TA}}^2$. So we neglect this small difference and use the Brillouin data to estimate the isothermal modulus:

$$K(P) = \rho\left(V_{\mathrm{LA}}^2 - \frac{4}{3}V_{\mathrm{TA}}^2\right). \tag{8}$$

Parameters K_0 and K_1 obtained by a linear fit of $K(P)$ are given in Table II. In the rest of the paper, we do not differentiate the isothermal and adiabatic bulk modulus, and only use the term "bulk modulus."

B. Change of the Brillouin and boson peak frequencies

Frequencies of the Brillouin modes, boson peak, and microscopic peak increase strongly with pressure in all the polymers studied here (Fig. 6). Variations of Brillouin modes (ν_{LA} and ν_{TA}) and of the microscopic peak are comparable in all polymers, supporting the assignment of the microscopic peak to sound-like modes. However, changes in ν_{BP} appear to be stronger than pressure-induced changes in ν_{LA}, ν_{TA}, and ν_{MP} (Fig. 6). Also, changes in the frequency of the longitudinal modes appear slightly larger than variations of the transverse modes in all polymers (Fig. 6). Apparently densification of the sample affects bulk modulus stronger than shear modulus.

Change of the mode frequency under pressure is often characterized by the Grüneisen parameter γ defined by the equation[43]

TABLE II. γ_{BP}, γ_{LA}, and γ_{TA} are Grüneisen parameters for the frequency of the boson peak, longitudinal, and transverse Brillouin modes, respectively. K_0 and K_1 are parameters of the linear expansion of the variation of the bulk modulus with pressure, $K(P)=K_0+K_1P$.

	γ_{LA}	γ_{TA}	γ_{BP}	K_0 (GPa)	K_1	γ_{TA}/K_1	γ_{BP}/K_1
PIB	3.88	3.46	5.02	7.31	9.16	0.38	0.55
PIP	3.45	2.9	4.35	5.62	8.66	0.33	0.50
PS	2.81	2.18	3.48	5.75	7.48	0.29	0.47
PMPS	3.44	2.7	5.41	5.31	8.73	0.31	0.62
PBD	3.97	3.36	4.92	4.89	9.12	0.37	0.54

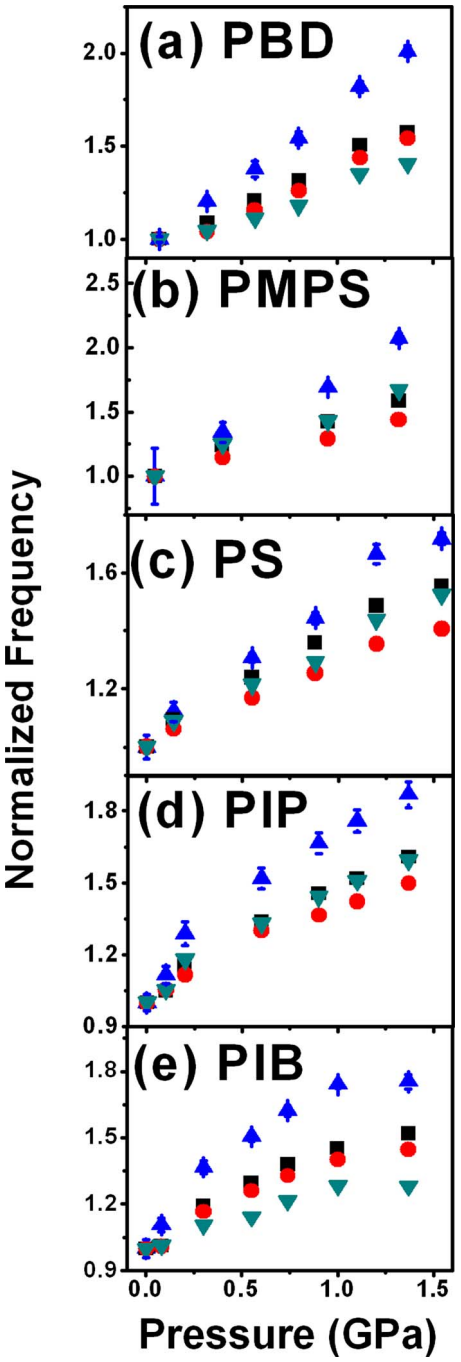

FIG. 6. (Color online) Pressure induced variations of vibrational frequencies at $T=140$ K in PBD (a), PMPS (b), PS (c), PIP (d), and PIB (e). All the frequencies are normalized to their values at initial pressure (see Table I). The symbols present: (▲)-boson peak; (▼)-microscopic peak; (■)-longitudinal modes, and (●)-transverse modes.

$$\gamma = \frac{\partial \ln \nu}{\partial \ln \rho}. \tag{9}$$

The values of the Grüneisen parameter for longitudinal and transverse Brillouin modes and for the boson peak frequency are given in Table II. For the pressure dependence of the mode frequency this gives after integration

$$\nu(P) = \nu_0(\rho(P)/\rho_0)^{\gamma}, \tag{10}$$

where the subscript zero means the value of the respective parameter at ambient pressure. Using the expression [Eq. (7)] for the pressure dependence of the density, we can rewrite Eq. (10):

$$\nu = \nu_0(1 + P/P_{01})^{\gamma/K_1} \tag{11}$$

with $P_{01}=K_0/K_1$. Thus any mode in first approximation is expected to have the power-law dependence on pressure. The difference in the pressure dependence of longitudinal and transverse modes and of the boson peak, as expected, also appears in the Grüneisen parameters (Table II): $\gamma_{BP} > \gamma_{LA} > \gamma_{TA}$. Typical values of γ_{BP} in Table II are between 4 and 5, γ_{TA} is around 3, and γ_{LA} is by 10%–20% larger than γ_{TA}. The estimated Grüneisen parameters for PIB differ from the earlier publication,[30] where pressure was applied at higher T, i.e., always in the liquid state. The exponent γ/K_1 in Eq. (11) is of the order of 0.3–0.4 for the transverse and longitudinal acoustic modes and ~0.5–0.6 for the boson peak.

According to the idea of simple homogeneous elastic continuum, all the sound-like modes should shift with pressure in a similar manner, just following changes in the sound velocity. This is indeed observed for longitudinal and transverse modes and also for the microscopic peak (Fig. 6). However, the frequency of the boson peak, which is in between the frequency of the Brillouin modes and of the microscopic peak, shifts much stronger in all polymers studied here. This result (Fig. 6) clearly demonstrates that the variation of the boson peak frequency with pressure does not follow the behavior expected for an elastic continuum. This conclusion agrees with earlier report for PIB,[30,31] and for network glasses SiO_2, GeO_2, and B_2O_3 (Ref. 28), and contradicts to the results observed in Ref. 14 for a $Na_2FeSi_3O_8$ glass.

Soft potential model (SPM) (Ref. 44) is currently the only model that provides clear predictions for the variations of the boson peak frequency under pressure. According to SPM predictions

$$\nu_{BP}(P) = \nu_{BP}(0)\left[1 + \frac{|P|}{P_0}\right]^{1/3}, \tag{12}$$

where P_0 is expressed via the bulk modulus K and two parameters of soft potentials: the strength of the random force f_0 between quasilocalized vibrations and a random deformation potential of the quasilocalized vibration Λ_0,[44]

$$P_0 = 3Kf_0/\Lambda_0. \tag{13}$$

It has been shown that Eq. (12) describes well the data for various glasses if P_0 is a constant.[27,44] Assuming P_0 constant, Eq. (12) also describes reasonably well the observed behavior of the boson peak frequency with pressure in all studied polymers here [Fig. 7(a)]. Equation (12) is actually similar to the general Eq. (11), but predicts the fixed value of the exponent ~0.33. This exponent is lower than the exponent $\gamma_{BP}/K_1 \sim 0.5–0.6$ obtained from the free fit of the data (Table II).

The model,[44] however, does not take into account variations of the elastic constants with pressure. Moreover, it is

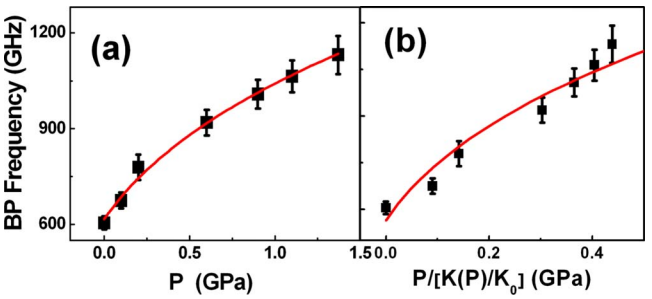

FIG. 7. (Color online) Pressure dependence of the boson peak frequency in PIP compared to the prediction of the soft potential model. Symbols are experimental data and lines are the fit: (a) The fit assumes P_0 is independent of pressure [Eq. (12)]; (b) The fit takes into account variations of the bulk modulus K [Eq. (14)]. Here K_0 is the bulk modulus at ambient pressure. Similar results have been obtained for all other polymers.

not obvious from the model whether P_0 should be a constant [as, e.g., P_{01} in Eq. (11) for sound waves] or it should correspond to actual values of parameters K, f_0, and Λ_0 at a current pressure. For example, the bulk modulus K increases significantly (up to a factor of 3) with pressure. We note that in the derivation of Eq. (12) the authors used the Hooke's linear law for the strain tensor, $\varepsilon''_{ik}=(P/3K)\delta_{ik}$.[44] It means that within this approximation the bulk modulus K should be taken at ambient conditions. We checked, however, whether Eq. (12) can describe the experimental data if one uses pressure-dependent bulk modulus in the expression for P_0 [Eq. (13)], while keeping parameters f_0 and Λ_0 constant, i.e., we use Eq. (12) in the form

$$\nu_{\mathrm{BP}}(P) = \nu_{\mathrm{BP}}(0)\left[1 + \frac{PK(0)}{aK(P)}\right]^{1/3}. \tag{14}$$

Here a is a constant and $K(P)$ is given by Eq. (8). Analysis of our data for ν_{BP} vs $PK(0)/K(P)$ shows clear disagreement of this function with the experimental data even on a qualitative level [Fig. 7(b)]: ν_{BP} increases with $PK(0)/K(P)$ superlinear, while Eq. (14) predicts sublinear behavior. Figure 7 shows data only for PIP, but the same is true for all other polymers studied here. Thus, SPM prediction for the boson peak frequency shift under pressure, Eq. (12), describes the experimental data only at constant P_0 that corresponds to approximations made for derivation of this expression in Ref. 44. It is not clear how strong variations of the elastic constants under pressure affect the prediction of SPM.

Many models relate the boson peak frequency to some kind of a characteristic length l (e.g., correlation length) in amorphous structure:[12,13,15–18,28]

$$\nu_{\mathrm{BP}} \propto \frac{V_{\mathrm{TA}}}{l}. \tag{15}$$

The transverse sound velocity is usually assumed because of the strong depolarization ratio of the boson peak in most of the studied glasses. In particular, recent computer simulations suggest that there is a characteristic length scale, below which homogeneous elastic continuum approximation for deformation breaks down and structural heterogeneity becomes important.[15–18] According to these studies, the characteristic length scale is related to the boson peak frequency through relationship (15). It has been also shown in these simulations[17,18] that the characteristic length scale l decreases with densification, indicating that the homogeneous elastic continuum works down to smaller length scales in densified glass. Moreover, the authors found an analytical relationship between the characteristic length and applied pressure: $l \propto P^{-1/4}$.

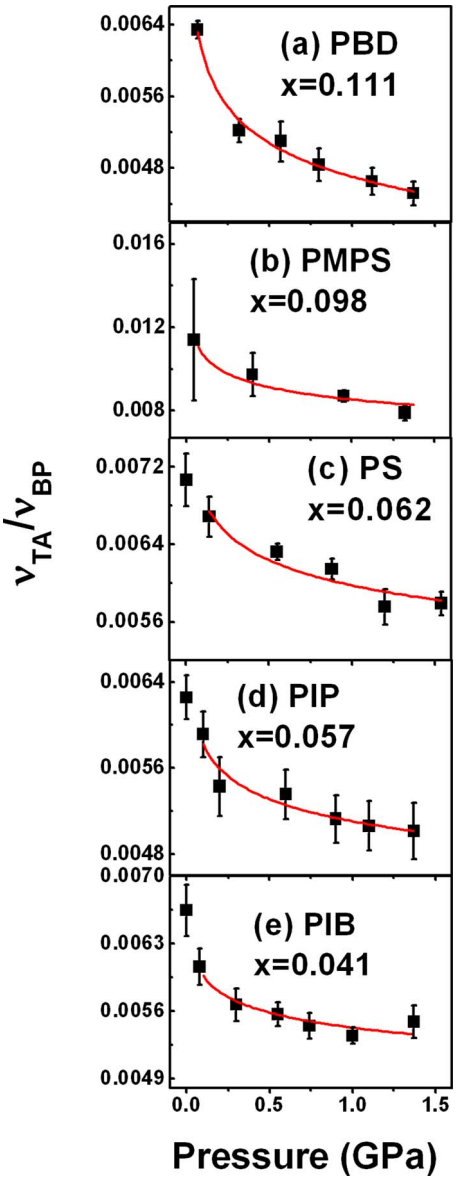

FIG. 8. (Color online) Pressure dependence of the ratio between frequency of the transverse Brillouin mode and the frequency of the boson peak at $T=140$ K: (a) PBD; (b) PMPS; (c) PS; (d) PIP; and (e) PIB. Symbols are experimental data and lines present the fits to a power law [Eq. (16)] with the ambient pressure point excluded from the fit; x is the value of the exponent obtained from the fit.

As we already emphasized above, our analysis shows that the boson peak frequency varies under pressure faster than longitudinal or transverse sound velocities (Fig. 6). In order to provide more quantitative analysis, Fig. 8 presents the experimental data for the pressure dependence of $\nu_{\mathrm{TA}}/\nu_{\mathrm{BP}}$.

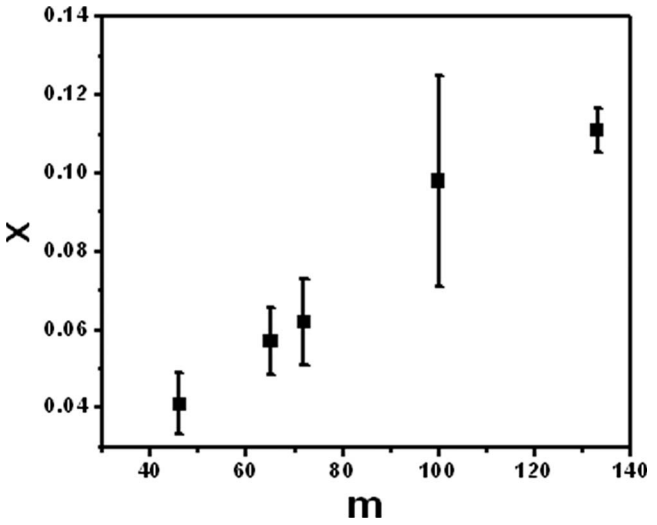

FIG. 9. The exponent x vs fragility m of the studied polymers. Fragility data are from Refs. 23 and 41.

According to many models,[12,13,15–18,28] change in the ratio ν_{TA}/ν_{BP} essentially reflects change in the characteristic length scale in the glassy structure [Eq. (15)]. All polymers studied here show significant decrease in the ratio with increase in pressure (Fig. 8), indicating a decrease in the characteristic length scale, in agreement with the prediction of simulations.[17,18] Following the simulations results, we analyzed the presented experimental data as a power-law dependence:

$$l \propto \frac{\nu_{TA}}{\nu_{BP}} \propto P^{-x}. \tag{16}$$

Here x is an exponent used as a free fit parameter. It is obvious that this power-law approximation works only at rather high pressure and cannot be extrapolated to the ambient pressure. So in our fit we used all the data excluding ambient pressure point, i.e., the fit starts from $P \sim 0.05-0.1$ GPa (Fig. 8). The so-obtained exponent varies from $x \sim 0.04$ in PIB up to $x \sim 0.1-0.11$ in PMPS and PBD (Fig. 8). All these values are significantly below the exponent $x \sim 0.25$ found in the simulation.[17,18] However, we should be cautious in this comparison because the simulations focus on soft-sphere packing at zero temperature, just above the onset of jamming, and the polymers considered here are far from that situation. Nevertheless, the presented analysis indeed confirms on a qualitative level that the results obtained from simulations and the observed stronger variations of the boson peak frequency might be related to pressure-induced variations in some characteristic length of the glassy structure.

It is interesting to note that exponent x seems to change with fragility of the material: It is the lowest in the least fragile PIB and the highest in PMPS and PBD, the most fragile among polymers studied here. Figure 9 indeed reveals some correlations between the exponent x and fragility index m of the polymers, and suggests that more fragile polymers have stronger variations of the ratio ν_{TA}/ν_{BP} with pressure. This suggestion is also confirmed by the analysis of the decrease in the ratio (Fig. 8): It drops $\sim 35-30\%$ in the case of PBD and PMPS, while it drops only $\sim 15-20\%$ in PIB and PIP in the comparable pressure range. This result is consistent with earlier report[45] that dynamics of more fragile systems is usually more sensitive to variations of density. These observations are very intriguing and invite some speculations. But we leave them out of the current paper.

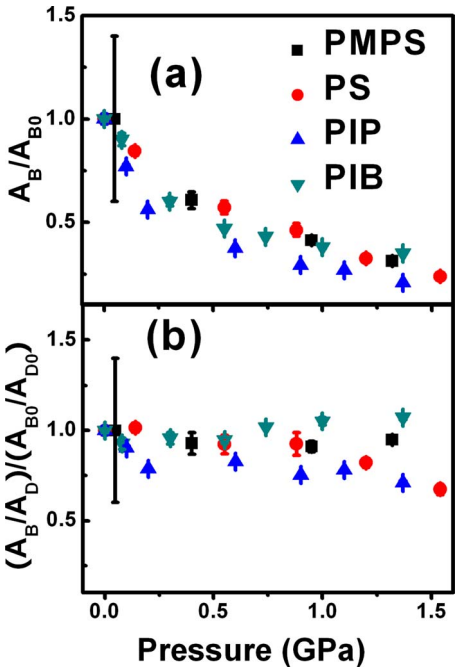

FIG. 10. (Color online) (a) Changes of the boson peak intensity under pressure in all studied polymers at $T=140$ K; (b) The same changes of the boson peak intensity scaled by the expected variations of the Debye level [Eq. (17)].

C. Variation of the boson peak amplitude

Amplitude of the boson peak is another important parameter that also changes significantly under pressure. According to the elastic continuum approximation the contribution of the sound-like modes should follow the Debye level, i.e., the strength of the boson peak relative to the Debye level, $A_{BP} = g(\nu_{max})/g_{Deb}(\nu_{max})$, should remain constant. This has been observed in inelastic nuclear scattering experiments in a densified $Na_2FeSi_3O_8$ glass.[14] However, an increase in A_{BP} under pressure has been reported from neutron scattering studies of PIB.[31]

Our data also show strong decrease ($\sim 3-5$ times) in the boson peak intensity under pressure for all studied polymers [Fig. 10(a)]. This decrease can be compared to a decrease expected for the Debye density of vibrational states. We stress that the chosen normalization of the light scattering intensity to the intensity of the optical modes (see Sec. II) here provides spectra per mole of the material. So the analysis of the Debye level variations should exclude density variations and can be estimated from the measured sound velocities:

$$A_{Debye} \propto \left(\frac{2}{V_{TA}^3} + \frac{1}{V_{LA}^3}\right). \tag{17}$$

Figure 10(b) compares the pressure-induced variations of the boson peak intensity to the expected variations of the Debye

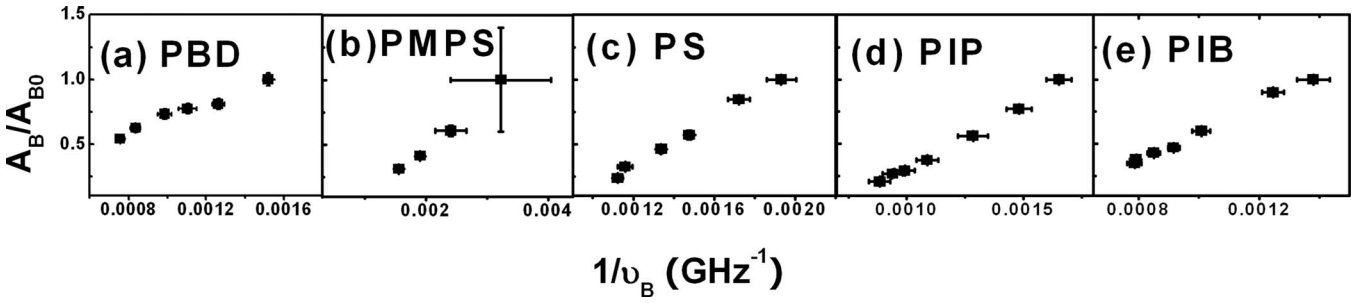

FIG. 11. Relationship between variations of the boson peak intensity and the inverse boson peak frequency at $T=140$ K: (a) PBD; (b) PMPS; (c) PS; (d) PIP; and (e) PIB.

level [Eq. (17)]. Figure 10(b) demonstrates that the latter is indeed the major factor in the observed decrease in the low-frequency peak intensity.

Unfortunately, it is not possible to provide more quantitative analysis of the boson peak amplitude from the light scattering data because of the so-called light-to-vibration coupling coefficient $C(\nu)$ (Ref. 46):

$$I_n(\nu) = C(\upsilon) \times \frac{g(\upsilon)}{\upsilon^2}. \tag{18}$$

It has been shown in our earlier studies that the coupling coefficient $C(\nu)$ decreases with pressure.[30] Thus, the measured decrease in the boson peak intensity is affected by additional variations of the coupling coefficient. One needs to analyze experimental data that measure directly the vibrational density of states $g(\nu)$ (e.g., neutron scattering data) in order to provide quantitative analysis of the variations of the strength of the boson peak A_{BP} under pressure. This analysis is important for testing of different models suggested for description of the boson peak. We are aware of only two papers with this kind of studies and they present contradicting conclusions.[14,31] Also, pressure-induced increase in the amplitude of the boson peak in the Raman spectra relative to the Debye level has been reported for a chalcogenide glass in Ref. 27. This result once again emphasizes that although change in the Debye level provides major variations in the decrease in the boson peak amplitude under pressure, the latter does not follow exactly the Debye level variations. It means that the elastic continuum approximation also fails in this case.

An unexpected observation reported in Ref. 31 is a relationship between the measurements in neutron scattering spectra amplitude of the boson peak, I_{BP}(neutrons) $=[g(\nu)/\nu^2]_{max}$, and the frequency of the boson peak: I_{BP}(neutrons)$^*\nu_{BP} \approx$ const. As it has been shown in Ref. 31, this observation is consistent with the SPM predictions. The reason is the one predicted at $\nu > \nu_{BP}$ proportionality of the density of vibrational states to frequency, $g(\nu)=D^*\nu$, with a prefactor D independent of pressure.[44]

As we already discussed above, the light scattering intensity does not provide direct measure of the vibrational density of states. Nevertheless, we analyzed the relationship between our measured variations of the boson peak intensity I_{BP} and of the inverse frequency of the boson peak (Fig. 11). Data for all polymers show some kind of a linear relationship

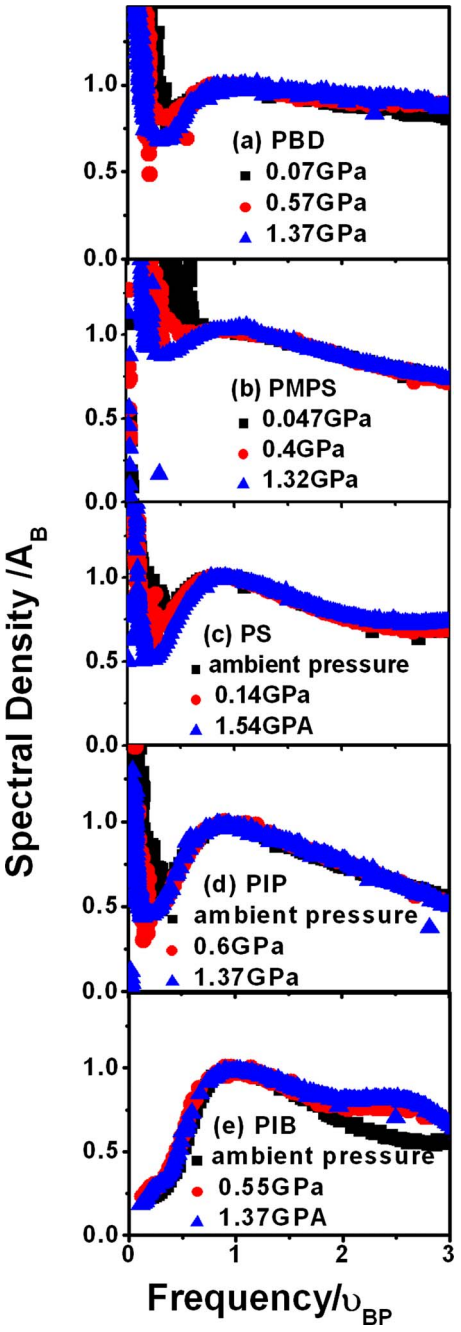

FIG. 12. (Color online) The spectra of the boson peak at different pressures scaled at the boson peak maximum: (a) PBD; (b) PMPS; (c) PS; (d) PIP; and (e) PIB.

between these two quantities, emphasizing that there might be a connection between the pressure-induced variations of the boson peak amplitude and frequency. Currently we cannot suggest any clear explanation for this observation.

We want to add a comment about a recent model of the boson peak proposed by Schirmacher and coworkers.[9–11] The model relates the boson peak to fluctuation of elastic constants in disordered structures. These fluctuations scatter acoustic-like modes and lead to their effective softening and appearance of the boson peak. Unfortunately, the model does not provide any predictions for the behavior of the boson peak under pressure that precludes analysis of our data in the framework of this model.

D. Spectral shape of the boson peak

It is known that the boson peak has rather universal spectral shape for many glass-forming systems.[47,48] This universality is lost in materials with low strength of the boson peak (A_{BP} is below 2).[13] In that case the vibrational density of states becomes closer to the expectations of the Debye model, and the boson peak appears to be broader.[13] Our earlier studies on PIB demonstrate[31] that despite significant ($\sim$2 times) decrease in the boson peak intensity and increase in the boson peak frequency under pressure, its spectral shape remains the same. We note that a different conclusion has been achieved in studies of chalcogenide glass in Ref. 27. However, the authors did not take into account the trivial Bose temperature factor, and the observed variation of the spectral shape of the boson peak might simply reflect the difference in thermal population of vibrational states at different frequencies.

We performed careful analysis of the light scattering spectra for the studied polymers. Spectral shape of the boson peak appears to be essentially independent of pressure (Fig. 12). Spectra of PMPS, PBD, and PS show some variations at frequencies below the boson peak. These variations are related to the strong quasielastic scattering (QES) in these polymers at ambient pressure. The quasielastic scattering intensity decreases significantly under pressure and causes the spectral changes observed at lower frequencies (Fig. 12). In the case of PIB, microscopic peak enters the high-frequency region and leads to the apparent variations of the high-frequency wing of the boson peak [Fig. 12(d)]. This analysis demonstrates that the spectral distribution of the modes around the boson peak remains the same even up to the pressure as high as 1.5 GPa. We achieved densification of the samples $\sim$12–17% (Fig. 5), changes in the boson peak frequency $\sim$2–2.5 times (Fig. 6), and variations in the boson peak amplitude 3–5 times [Fig. 10(a)], but the spectral shape of the peak remains essentially unaffected. This observation emphasizes some universality in the spectral distribution of the vibrational modes around the boson peak that should be taken into account by any model that attempts to describe the boson peak.

V. CONCLUSION

We presented detailed light scattering studies of the influence of pressure on the boson peak in five different polymers. In all cases we observed that the pressure-induced shift of the boson peak frequency is significantly stronger than variations of the sound modes and of the microscopic peaks. This observation disagrees with the expectations of a simple elastic continuum variation. It is consistent, however, with the results of recent simulations[15–18] that suggest decrease in characteristic length scale in a disordered structure under densification. We demonstrate that the main variation of the boson peak amplitude might be ascribed to the pressure-induced variations of the Debye level. However, we cannot perform more accurate quantitative analysis of the boson peak amplitude variations because light scattering does not provide direct measure of the vibrational density of states. We also demonstrate that the spectral shape of the boson peak remains essentially independent of pressure despite significant changes in the peak frequency and amplitude. Comparison of our results to predictions of different models illustrates that soft potential model is consistent with our data, although it should take into account significant variations of elastic constants under pressure. It is difficult to judge other models because they don't provide quantitative predictions for the pressure dependence of the boson peak. Our analysis also reveals a few unexpected observations: (i) there might be a connection between the pressure-induced variations of the boson peak amplitude and of the boson peak frequency and (ii) there might be some correlations in variations of the materials properties (density, fast dynamics) under pressure and its initial fragility. These observations deserve additional experimental and theoretical studies and might help to shed additional light on the microscopic nature of the boson peak vibrations.

ACKNOWLEDGMENTS

Akron team acknowledges the financial support from NSF Polymer program (Grant Nos. DMR-0605784 and DMR-0804571). V.N.N. thanks RFBR Grant No. 06-02-16172.

*Author to whom correspondence should be addressed.
alexei@uakron.edu

[1] *Amorphous Solids: Low-Temperature Properties*, edited by W. A. Phillips (Springer-Verlag, Berlin, 1981).
[2] G. Winterling, Phys. Rev. B **12**, 2432 (1975).
[3] U. Buchenau, H. M. Zhou, N. Nucker, K. S. Gilroy, and W. A. Phillips, Phys. Rev. Lett. **60**, 1318 (1988).
[4] A. P. Sokolov, V. N. Novikov, and B. Strube, Europhys. Lett. **38**, 49 (1997).
[5] V. L. Gurevich, D. A. Parshin, J. Pelous, and H. R. Schober, Phys. Rev. B **48**, 16318 (1993).
[6] V. L. Gurevich, D. A. Parshin, and H. R. Schober, Phys. Rev. B

67, 094203 (2003).
[7] D. A. Parshin, H. R. Schober, and V. L. Gurevich, Phys. Rev. B **76**, 064206 (2007).
[8] A. V. Granato, Physica B **219–220**, 270 (1996).
[9] E. Maurer and W. Schirmacher, J. Low Temp. Phys. **137**, 453 (2004).
[10] W. Schirmacher, Europhys. Lett. **73**, 892 (2006).
[11] W. Schirmacher, G. Ruocco, and T. Scopigno, Phys. Rev. Lett. **98**, 025501 (2007).
[12] E. Duval, A. Boukenter, and T. Achibat, J. Phys.: Condens. Matter **2**, 10227 (1990).
[13] A. P. Sokolov, R. Calemczuk, B. Salce, A. Kisliuk, D. Quitmann, and E. Duval, Phys. Rev. Lett. **78**, 2405 (1997).
[14] A. Monaco, A. I. Chumakov, G. Monaco, W. A. Crichton, A. Meyer, L. Comez, D. Fioretto, J. Korecki, and R. Ruffer, Phys. Rev. Lett. **97**, 135501 (2006).
[15] F. Leonforte, A. Tanguy, J. P. Wittmer, and J.-L. Barrat, Phys. Rev. Lett. **97**, 055501 (2006).
[16] F. Leonforte, R. Boissiere, A. Tanguy, J. P. Wittmer, and J.-L. Barrat, Phys. Rev. B **72**, 224206 (2005).
[17] M. Wyart, L. E. Silbert, S. R. Nagel, and T. A. Witten, Phys. Rev. E **72**, 051306 (2005).
[18] L. E. Silbert, A. J. Liu, and S. R. Nagel, Phys. Rev. Lett. **95**, 098301 (2005).
[19] V. N. Novikov, Y. Ding, and A. P. Sokolov, Phys. Rev. E **71**, 061501 (2005).
[20] L. E. Bove, C. Petrillo, A. Fontana, and A. P. Sokolov, J. Chem. Phys. **128**, 184502 (2008).
[21] J. S. Spells and I. W. Shepherd, J. Chem. Phys. **66**, 1427 (1977).
[22] B. Frick, G. Dosseh, A. Cailliaux, and C. Alba-Simionesco, Chem. Phys. **292**, 311 (2003).
[23] Y. F. Ding, V. N. Novikov, A. P. Sokolov, A. Cailliaux, C. Dalle-Ferrier, C. Alba-Simionesco, and B. Frick, Macromolecules **37**, 9264 (2004).
[24] S. L. Isakov, S. N. Ishmaev, V. K. Malinovsky, V. N. Novikov, P. P. Parshin, S. N. Popov, A. P. Sokolov, and M. G. Zemlyanov, Solid State Commun. **86**, 123 (1993).
[25] C. Levelut, N. Gaimes, F. Terki, G. Cohen-Solal, J. Pelous, and R. Vacher, Phys. Rev. B **51**, 8606 (1995).
[26] A. Monaco, A. I. Chumakov, Y.-Z. Yue, G. Monaco, L. Comez, D. Fioretto, W. A. Crichton, and R. Ruffer, Phys. Rev. Lett. **96**, 205502 (2006).
[27] K. S. Andrikopoulos, D. Christofilos, G. A. Kourouklis, and S. N. Yannopoulos, J. Non-Cryst. Solids **352**, 4594 (2006).
[28] J. Schroeder, W. M. Wu, J. L. Apkarian, M. Lee, L. Hwa, and C. T. Moynihan, J. Non-Cryst. Solids **349**, 88 (2004).
[29] M. Yamaguchi, T. Nakayama, and T. Yagi, Physica B **263–264**, 258 (1999).
[30] B. Begen, A. Kisliuk, V. N. Novikov, A. P. Sokolov, K. Niss, A. Chauty-Cailliaux, C. Alba-Siminoesco, and B. Frick, J. Non-Cryst. Solids **352**, 4583 (2006).
[31] K. Niss, B. Begen, B. Frick, J. Ollivier, A. Beraud, A. P. Sokolov, V. N. Novikov, and C. Alba-Simionesco, Phys. Rev. Lett. **99**, 055502 (2007).
[32] B. Frick and C. Alba-Simionesco, Appl. Phys. A: Mater. Sci. Process. **74**, S549 (2002).
[33] C. H. Whitfield, E. M. Brody, and W. A. Bassett, Rev. Sci. Instrum. **47**, 942 (1976).
[34] V. K. Malinovsky, V. N. Novikov, and A. P. Sokolov, Phys. Lett. A **153**, 63 (1991).
[35] J. M. Brown, L. J. Slutsky, K. A. Nelson, and L.-T. Cheng, Science **241**, 65 (1988).
[36] G. Beaucage, R. Composto, and R. S. Stein, J. Polym. Sci., Part B: Polym. Phys. **31**, 319 (1993).
[37] U. Gaur and B. Wunderlich, J. Phys. Chem. Ref. Data **11**, 313 (1982).
[38] R. F. Boyer and R. Simha, J. Polym. Sci., Polym. Lett. Ed. **11**, 33 (1973).
[39] J. Dudowicz, K. F. Freed, and J. F. Douglas, J. Phys. Chem. B **109**, 21285 (2005).
[40] R. Zorn, G. B. McKenna, L. Willner, and D. Richter, Macromolecules **28**, 8552 (1995).
[41] R. Bohmer, K. L. Ngai, C. A. Angell, and D. J. Plazek, J. Chem. Phys. **99**, 4201 (1993).
[42] K. Kunal, M. Paluch, C. M. Roland, J. E. Puskas, Y. Chen, and A. P. Sokolov, J. Polym. Sci., Part B: Polym. Phys. **46**, 1390 (2008).
[43] C. Kittel, *Introduction to Solid State Physics*, 7th ed. (Wiley, New York, 1996), p. 139.
[44] V. L. Gurevich, D. A. Parshin, and H. R. Schober, Phys. Rev. B **71**, 014209 (2005).
[45] C. Alba-Simionesco, A. Cailliaux-Chauty, A. Alegria, and G. Tarjus, Europhys. Lett. **68**, 58 (2004).
[46] R. Shuker and R. W. Gammon, Phys. Rev. Lett. **25**, 222 (1970).
[47] V. K. Malinovsky and A. P. Sokolov, Solid State Commun. **57**, 757 (1986).
[48] V. K. Malinovsky, V. N. Novikov, P. P. Parshin, A. P. Sokolov, and M. G. Zemlyanov, Europhys. Lett. **11**, 43 (1990).